Arch. Metall. Mater. **68** (2023), 1, 307-317

DOI: https://doi.org/10.24425/amm.2023.141507

N.M. ANAS[1], S.A. ZAKARIA[1], A.S. ANASYIDA[1*], H. MOHAMAD[1], B.K. DHINDAW[2]

# INFLUENCE OF SEMISOLID AND STRONTIUM ADDITION ON DRY SLIDING WEAR BEHAVIOR OF HYPOEUTECTIC Al-Si ALLOY

The study aims to investigate the effect of semisolid structure and strontium (Sr) addition on the wear behavior of hypoeutectic Al-Si alloy. Semisolid hypoeutectic Al-Si alloy was prepared using cooling slope casting with addition of 0 to 0.93 wt.% Sr. Microstructural study was done using an optical microscope. Vicker microhardness and pin on disc tribometer were used for microhardness and wear testing. When compared to conventional casting, the microhardness of the semisolid hypoeutectic Al-Si alloy improved by 9.8%. Sr addition at 0.43 wt.% resulted in a refined eutectic structure with a 17% increase in hardness over conventional casting. The globular structure α-Al formed during semisolid casting reduced porosity, and the addition of Sr refined the eutectic silicon into a fine fibrous structure that is tightly bound with the Al matrix. These are the primary factors that contribute to the high wear resistance in modified-Sr semisolid alloys.

*Keywords:* Hypoeutectic Al-Si alloy; semisolid; cooling slope; Sr; wear resistance

## 1. Introduction

Hypoeutectic Al-Si alloys offer good wear resistance, high strength, high hardness, and low thermal expansion together with excellent castability [1-4]. In addition, their reduced density makes these alloys very competitive in wear applications [5,6]. Hypoeutectic Al-Si alloys are extensively used in marine castings, motor cars and lorry fittings/pistons and engine parts, cylinder blocks and heads, cylinder liners, axles and wheels, rocker arms, automotive transmission casings, water cooled manifolds and jackets, piston for internal combustion engines, pump parts, high speed rotating parts and impellers [7,8]. The in-service performance of the hypoeutectic Al-Si alloy castings primarily depends on their microstructures. The eutectic microstructure present in the inter dendritic region of Al-Si alloy determines the mechanical properties of the Al-Si alloys because the eutectic phase contains a hard, brittle silicon phase in a softer $\alpha$-Al phase [5,9]. The use of Al-Si alloys in conventional cast grades has been restricted due to high latent heat and long solidification time which results in segregation and excessive growth of primary silicon particles, and unfavorable shrinkage behavior [10]. Therefore, a new approach method should be evaluated to overcome this problem.

Semisolid was recently considered to be a viable alternative route in the production of these alloys, as it can help to overcome the drawbacks. In semi-solid metal (SSM) processing, the casting temperature and heat content are much reduced, thus coarsening of the primary silicon and shrinkage are minimized [11]. The main attention of semi-solid metal (SSM) processing on aluminium alloy is to achieve globular structure of the primary Al phase to improve mechanical properties and thixotropic behaviour of the alloys [12]. This is important during die filling where more globular and finer particles lead to better flow behavior. One of the convenient and industrially viable low-cost semi-solid processing routes is by preparing liquid melt using inclined slopes also called "slurry on demand" processing [11,13]. Lasa and Rodriguez-Ibabe [14] have found the improvements in wear behaviour of thixoformed hypoeutectic Al-Si alloy compared to conventional cast alloy with similar composition. This was attributed to the fine, homogeneous and globular microstructure in thixoformed alloys. Studies conducted by Alhawari et al. [15] have stated that wear behaviour of thixoformed A319 alloy was found to be lower than that of as-cast A319 alloy. This is believed to be due to the increased hardness, finer grain size, uniform distribution of silicon and intermetallic phases and reduction in porosity level. In addition, Agarwal and Srivastava [16] reported

[1] UNIVERSITI SAINS MALAYSIA, STRUCTURAL NICHE AREA. SCHOOL OF MATERIALS & MINERAL RESOURCES ENGINEERING, ENGINEERING CAMPUS, MALAYSIA 14300 NIBONG TEBAL, PULAU PINANG
[2] INDIAN INSTITUTE OF TECHNOLOGY KHARAGPUR 721302, INDIA

* Corresponding Author: anasyida@usm.my

that Al-Si LM6 alloy fabricated by semi-solid casting possesses good adhesive wear properties and resistance against the harder counter surfaces. Shehata et al. [17] found that the tribological performance of A390 semisolid alloy using cooling slope plate (CSP) has lower weight loss and higher friction coefficient compared to the conventionally cast specimens.

Furthermore, the shape and distribution of silicon particles in eutectic Al-Si, as well as in the alloy matrix influence the tribological properties of hypoeutectic Al-Si alloys. This is due to the fact that the equilibrium solid solubility of Si in the Al matrix is only 0.05 wt.% at room temperature. As a result, when the Si content in Al alloys exceeds 0.05 wt.%, the amount of Si in non-solid solution is greater than the amount of Si in solid solution. The majority of nonsolid solution Si exists as eutectic Si. The Sr modification process is widely used to treat Al-Si alloys because Sr can efficiently transform the eutectic Si phases from coarse flaky structure to fine fibrous structure and improve the mechanical properties of AlSi alloys [18].

It has been reported that the modification of eutectic Al-Si alloy has little influence on wear resistance [19]. On the other hand, Prasad et al. [20] have observed that the shape and size of the silicon particles are controlling factors in the formation of cracks and wear resistance, and that the cracking tendency increases with the size of the silicon particles in the Al-Si alloys. In addition, Yang et al. [21] have claimed that the addition of chemical modifiers Sr and Sb modified the morphology of eutectic Si particles and further improved the wear resistance of A357 alloy. Other studies [22] also have reported that Sr exhibits a relatively good modification effect and lasts long. Thus, the present work was undertaken to study the effect of combined semisolid and modifier on wear properties of hypoeutectic Al-Si aluminium alloy.

## 2. Experimental procedure

Hypoeutectic Al-Si alloy was used in the investigation. The hypoeutectic Al-Si alloy was cut into a smaller piece and added in the graphite crucible. Melting was carried out in an electrical resistance furnace at 800°C. The melting temperature was kept at 800°C for 30 minutes. Strontium was added as the modifier in the form of Al-10wt.% Sr master alloy with addition of 0.5, 1.0 and 1.5 wt.%. The molten alloy was stirred at 800°C using a stirrer to homogenize the molten mixture and then temperature was reduced to 680°C and held for 30 minutes. The layer slag formed at top was skimmed and removed. The melts were then poured onto a steel slope and flow down into a pre-heated steel mould (300°C). The parameters for slope casting are; slope angle of 60°, cooling slope distance of 200 mm and pouring temperature 680°C. The sample was left to be cooled down at room temperature for 30 minutes producing samples 14 mm in diameter and 80 mm in length. The chemical composition of semisolid hypoeutectic Al-Si alloy without and with addition of Sr was measured by X-ray fluorescent (XRF) diffractometer and is shown in TABLE 1.

TABLE 1

Chemical composition of semisolid hypoeutectic Al-Si alloy without and with Sr addition

| Sample | Composition (wt.%) | | | | |
|---|---|---|---|---|---|
| | Al | Si | Mg | Fe | Sr |
| Hypoeutectic Al-Si | 92.7547 | 6.3986 | 0.3183 | 0.2253 | — |
| Hypoeutectic Al-Si-0.5% Al-10Sr | 92.0389 | 6.6908 | 0.3726 | 0.2594 | 0.4301 |
| Hypoeutectic Al-Si-1.0% Al-10Sr | 92.5666 | 6.2447 | 0.2573 | 0.2384 | 0.6261 |
| Hypoeutectic Al-Si-1.5% Al-10Sr | 92.2458 | 6.3317 | 0.3424 | 0.2852 | 0.9278 |

Optical microscope was used to observe the microstructure of the etched samples. The samples were etched using Keller's reagent for 10 seconds. Microhardness test was carried out using Vicker microhardness at a load of 0.5 kg at 10 different regions. The wear test was performed on pin-on-disc (TR 20 DUCOM). In the wear test, the flat end of a cylindrical specimen 10 mm in diameter and 20 mm in length was fixed in clamp to prevent the sample from rotating during the test. The pin and disc were cleaned ultrasonically by using acetone and were dried before the test. The wear test was carried out at room temperatures and at dry condition. The standard disc was made of hard steel EN31 (Fe-2.3%Cr-0.9%C) with a hardness of 62 HRC (provided by DUCOM). The dry sliding wear experiments were conducted at a fixed speed of 1 m/s in dry conditions at room temperature of 25°C. The diameter of the rounded track traversed by the pin was fixed at 100 mm for all tests. Three different axial loads of 10 N, 30 N and 50 N were applied to the pins against the plane surface of the rotating disc for a sliding distance up to 5000 m. The test is interrupted for measurement at 1000 m, 2000 m, 3000 m, 4000 m, and 5000 m sliding distances. The weight loss of the pin material was measured prior ($W1$) and after ($W2$) the wear test using a digital weight balance up to accuracy of 0.0001 g. The weight loss was then converted to volume loss. Each experiment was repeated at least three times. Volume loss ($VL$) and specific wear rate ($SWR$) were calculated using Eq. (1) and Eq. (2), respectively [23].

$$VL = \Delta W/\rho \tag{1}$$

$$SWR = VL/NS \tag{2}$$

Where $VL$ is the volume loss ($mm^3$); $SWR$, the specific wear rate ($mm^3$/N m); $\Delta W$, the weight loss = ($W1$–$W2$); $\rho$, the density ($g/cm^3$); $N$, the applied load (N); and $S$, the sliding distance (m).

Friction coefficient values under steady state were calculated by the load cell attached with the apparatus. The worn surfaces were observed using FESEM (SURPA 35VP ZEISS) equipped with an additional Energy Dispersive X-Ray (EDX).

## 3. Results and discussion

### 3.1. Microstructure

Fig. 1 shows microstructure of conventional hypoeutectic Al-Si alloy and semisolid hypoeutectic Al-Si alloy with addition of 0, 0.43, 0.60 and 0.93 wt.% Sr. In Fig. 1(a), the unmodified hypoeutectic Al-Si alloy using conventional casting showed a dendrite structure of α-Al with coarse eutectic Si structure. While in Fig. 1(b), α-Al appeared as globular structure and eutectic Si remained as coarse structure in semisolid casting. In contrast, Sr-modified semisolid hypoeutectic alloy with addition of Sr refined the eutectic structure of Al-Si alloy to fibrous morphology. According to Jigajinni et al. [24], addition of strontium only affects the morphology of the eutectic silicon without altering the α-Al phase. By increasing the amount of Sr from 0.43 wt.% to 0.93 wt.%, eutectic structure was further refined. Sr block and needle shaped intermetallic phase was detected in alloys containing more than 0.63 wt.% Sr. The needle shaped intermetallic phase containing Sr was confirmed as $Al_2Sr$ by XRD analysis as shown in Fig. 2. At this range, the addition of Sr can be classified as over-modification. Over-modification can easily be detected by segregation of Sr based compounds at eutectic silicon regions forming $Al_2Si_2Sr$ [24,25].

Fig. 3 shows the back scattered and EDX analysis of semisolid hypoeutectic Al-Si alloys with 0.63 wt.% Sr. The EDX result of six different points were summarized in TABLE 2. The bright contrast block (A) is the strontium intermetallic phases which contain 46.96 wt.% Sr and high possibility can be assumed as $Al_2Si_2Sr$ phase. However, XRD analysis results unable to detect the pattern of $Al_2Si_2Sr$ phase. This may be due to low percentage of phases present in the alloy. Light gray-

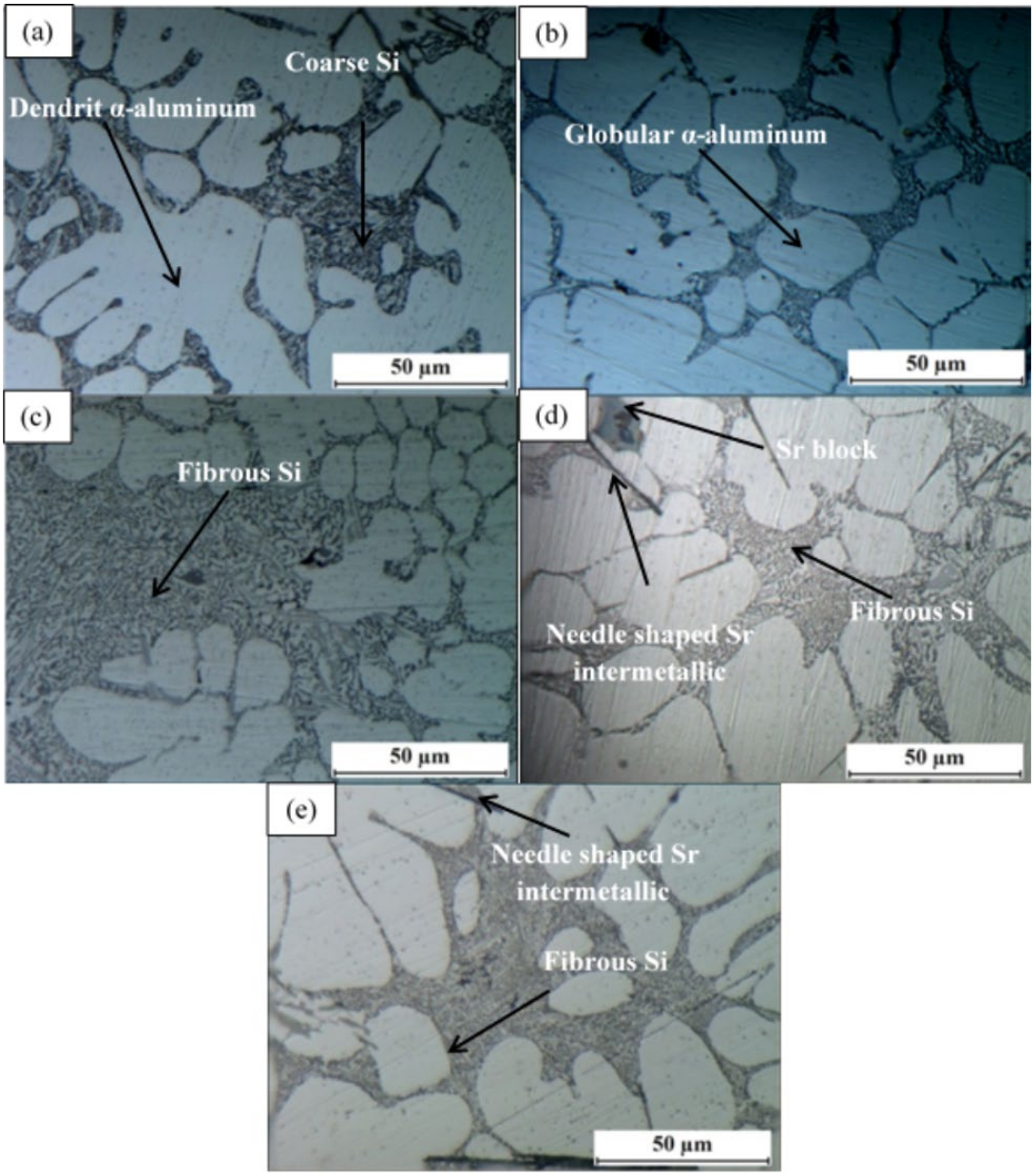


Fig. 1. Optical micrographs of hypoeutectic (a) conventional A-Si alloy without Sr added and semisolid hypoeutectic Al-Si alloys added with different wt.% of Sr (b) 0 wt.% Sr, (c) 0.43 wt.% Sr, (d) 0.63 wt.% Sr and (e) 0.93 wt.% Sr

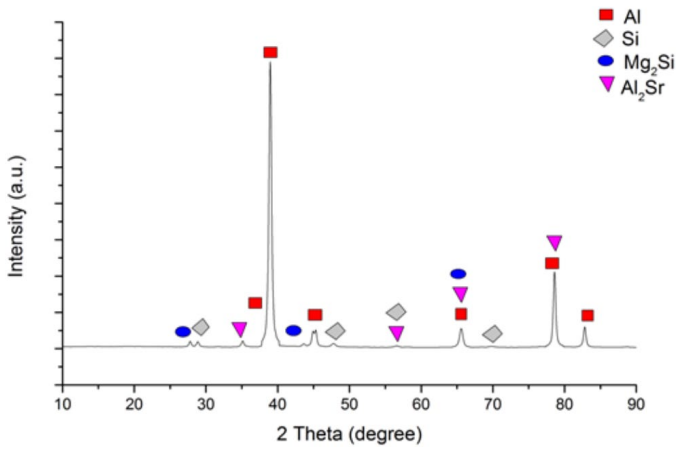


Fig. 2. XRD analysis of hypoeutectic Al-Si alloy containing 0.93 wt.% Sr

ish region (B) contains magnesium element. In Al-Si alloys, magnesium usually formed as $Mg_2Si$ phase as confirmed by XRD analysis. EDX analysis in Region C revealed high silicon

TABLE 2

EDX analysis of semisolid hypoeutectic Al-Si alloys with 0.63 wt.% Sr

| Location | Element (wt.%) | | | | |
|---|---|---|---|---|---|
| | Al | Si | Sr | Mg | Fe |
| A (Bright contrast region) | 24.25 | 31.79 | 46.96 | — | — |
| B (Light grayish region) | 61.10 | 27.65 | — | 11.25 | — |
| C (Dark contrast region) | 36.47 | 63.53 | — | — | — |
| D (Grayish background) | 95.71 | 4.29 | — | — | — |
| E (Bright contrast region) | 52.57 | 25.7 | — | — | 21.73 |
| F (Gray region) | 66.10 | 33.9 | — | — | — |

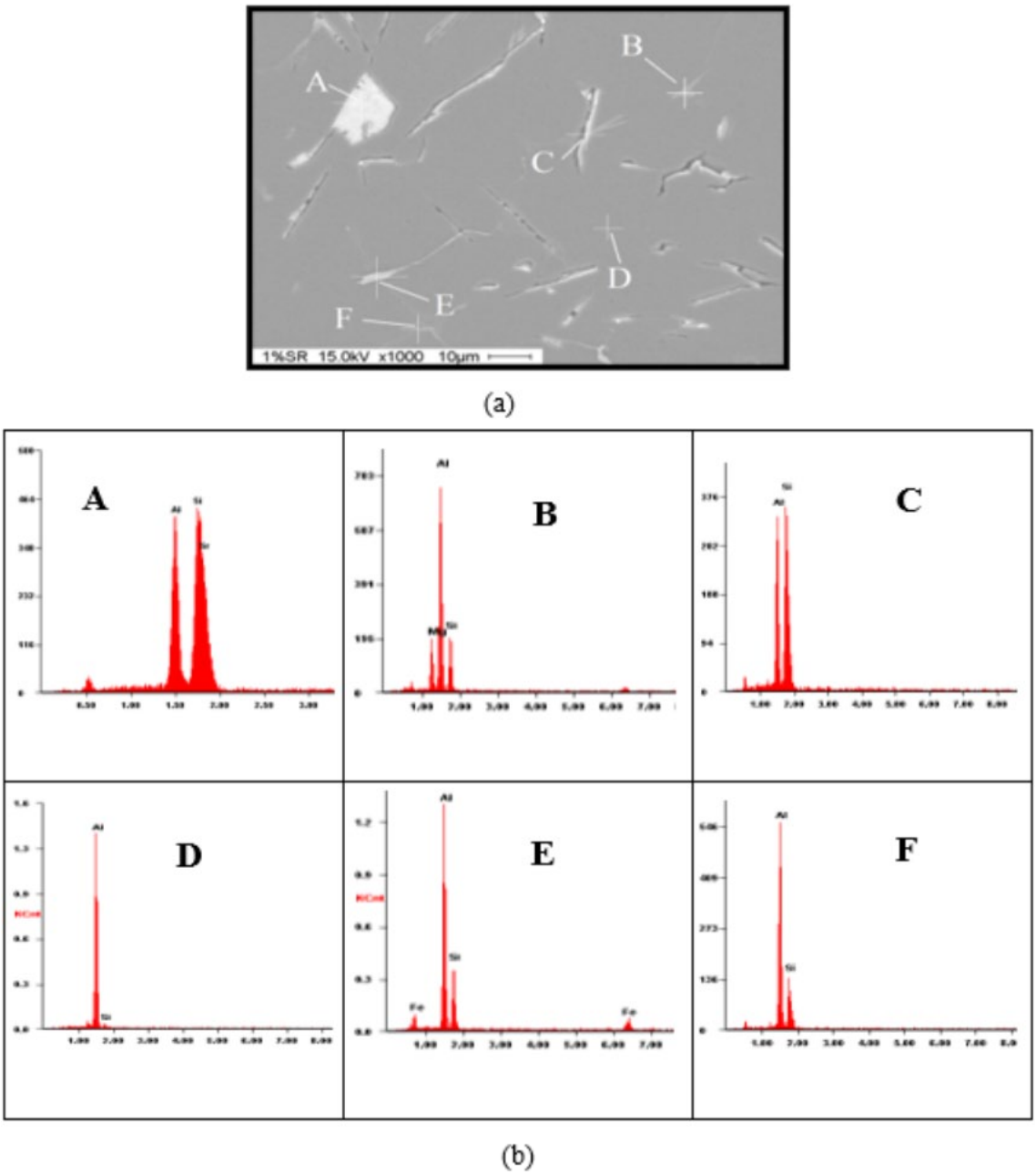


Fig. 3 Semisolid hypoeutectic Al-Si alloys with 0.63 wt.% Sr, (a) back scattered micrograph and (b) EDX spectrum

content which draws the possibility of silicon phase. Region D and F can be identified as alpha aluminum phase due to higher Al content. The bright contrast region labelled as E has moderate iron presence, probably intermetallic phases of iron, β-$Al_5FeSi$ [26].

### 3.2. Microhardness

Fig. 4 shows the Vickers microhardness of semisolid hypoeutectic Al-Si alloy with different strontium addition of 0 wt.% to 0.93 wt.%. Microhardness of hypoeutectic Al-Si alloy using conventional casting recorded a value of 55 HV. While semisolid hypoeutectic Al-Si alloy recorded a value of 60.4 HV, which is approximately 9.8% higher than conventional casting.

It can be noted from Fig. 4 that the hardness value for semisolid alloy increases with addition of Sr up to 0.43 wt.% Sr with value of 64.7 HV. The increase in hardness was due to the refinement of Si phase in the eutectic phase and globular structure of α-Al formed during semisolid casting that may reduce the porosity [27]. When compared to conventional casting, the combination of globular structure and refined eutectic structure produced by semisolid casting and the addition of modifier increased the hardness by 17.64%. Further addition of Sr up to 0.93 wt.% slightly decreased the hardness of the alloys from 64.7 Hv to 60.2 Hv. This may be due to coarsening of Sr block and needle shaped intermetallic phases in in the alloy.

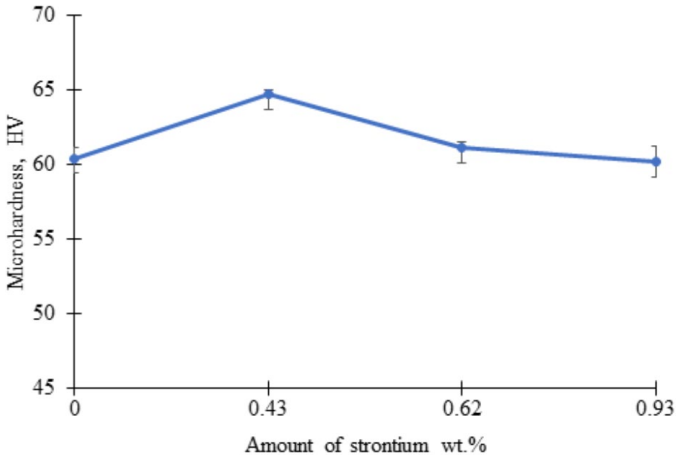


Fig. 4. Microhardness of conventional and slope cast alloy with various amount of strontium

### 3.3. Wear Behaviour

#### 3.3.1. Volume loss

Pin on disc wear test was conducted to evaluate the effect of semisolid processing and addition of Sr on hypoeutectic Al-Si alloy. Fig. 5 to Fig. 7 present volume loss as a function of the sliding distances for all the samples. It can be observed that the volume loss of the alloys increases linearly with increasing sliding distances. Increasing volume loss is usual with normal applied load, and this is in agreement with others research [28,29]. This is due to more interaction between the sample and the wear track surface as the sliding distance increases [30]. It can be implied that wear loss is directly proportional to sliding distance. At lower load, the volume loss only contributed by oxide layer formation at wear surface and wear rate is low. But, at higher load, friction arises and further plastic deformation, progressive debonding and fracture of surface, thus wear rate is high. Various parameters have been studied by [31] and they have concluded that wear behavior of aluminum alloys are dependent on alloy composition, mechanical properties (hardness, plasticity, ductility), sliding speed, sliding distance and normal pressure.

The performance of hypoeutectic Al-Si alloys primarily depends on their microstructures, especially α-Al in hypoeutectic alloy. Fine equiaxed Al and eutectic Si ensures improved mechanical properties, good tribological features and uniform distribution of second phase particles enhance its machinability [32]. Copious nucleation mechanisms in slope casting are able to produce globular Al phase surrounded by eutectic silicon matrix and produce better wear properties than conventional casting methods.

Conventional hypoeutectic A1-Si alloy has higher volume loss than those unmodified semisolid and semisolid strontium modified alloys. Studies conducted by Chandrashekharaiah et al. [31] 2009 have reported that the addition of grain refiner and modifier on hypoeutectic Al-Si alloys resulted in less wear rate at longer sliding distances. Clearly, the strontium modifier does refine the eutectic silicon into a fine fibrous structure that is strongly bounded by the Al matrix in their position to resist the destructive wear action of the abrasive particles. The strong matrix reduces the plastic deformation and ploughing action of asperities among the wear surface. The unmodified conventional and unmodified semisolid hypoeutectic Al-Si alloys usually consist of coarse needle like shape silicon phase that can easily become crack initiation sites. Thus, refined primary silicon phase and eutectic silicon phase assist in suppressing crack initiation and propagation and contribute to lower wear loss [32]. These results showed that changes in the microstructure formed by semisolid processing and addition of modifier had affected the wear resistance.

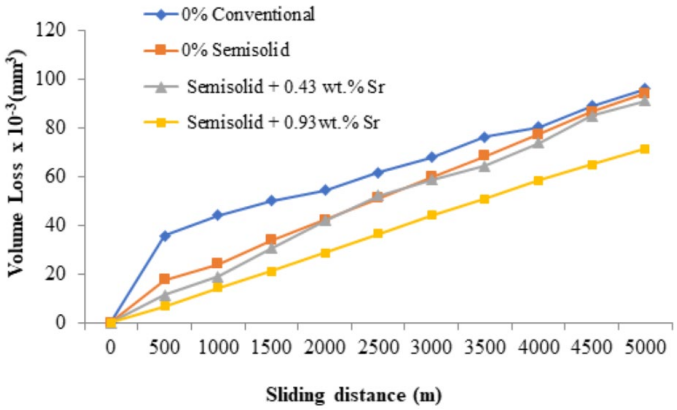


Fig. 5. Volume loss as a function of sliding distances of different types of samples at applied load of 10 N

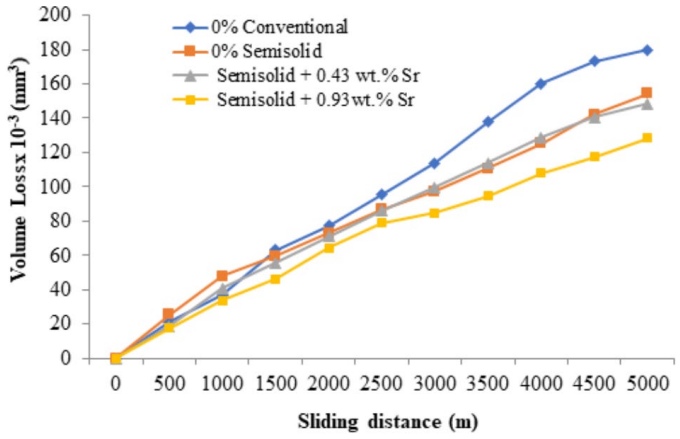


Fig. 6. Volume loss as a function of sliding distances of different types of samples at applied load of 30 N

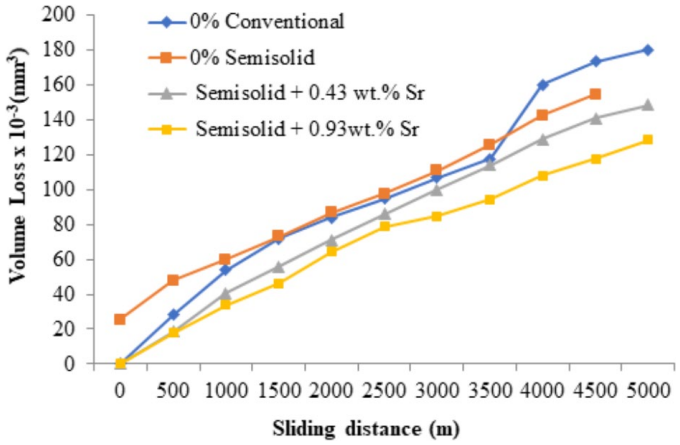


Fig. 7. Volume loss as a function of sliding distances of different types of samples at applied load of 50 N

### 3.3.2. Specific wear rate, K'

Fig. 8 depicts the specific wear rate of conventional hypoeutectic Al-Si alloy and semisolid hypoeutectic Al-Si alloy with varying amounts of strontium added at various applied loads. The specific wear rate decreases as load increases, indicating a lower wear rate at high load. This finding was due to the reinforcement of the transferred layers from the samples and the counter disc surface material. At high load (50 N), there is a large volume loss in the form of debris at the surface of the worn sample (Fig. 7). These small particles can be easily oxidized, hated, and sintered to cover the worn surface. It re-adhered on the surface of the sample due to friction between the sample and the counter disc, improving wear resistance at high loads. It can be seen that the semisolid alloy showed superior wear performance than conventionally cast samples. This is due to the distribution and smaller size of Si particles, as well as the reduction in porosity and improved soundness caused by semi-solid processing [33]. In the Sr-modified alloy, small and spherical silicon particles protected the surface from wear and lead to less material damage [21]. However, the coarser silicon particles in conventional alloy with larger aspect ratio tend to fracture more easily resulting in higher wear rate through abrasion. Furthermore, the refinement and homogenization of the intermetallic phases containing Sr which act as effective load-bearing elements were beneficial in enhancing the wear resistance since they have good interfacial bonding with the matrix [17]. The presence of spherical silicon particles and intermetallic phases with addition of Sr influenced the hardenability of semisolid alloy and depth of the subsurface deformation which reduces the specific wear rate [27]. The sample with 0.93 wt.% Sr has the lowest specific wear rate. A lower specific wear rate indicates that the material is more resistant to wear [34]. The probability of producing wear regimes was based on the K' value range, according to Rabinowicz [35]. Semisolid hypoeutectic Al-Si alloys, both unmodified and modified, fall under the moderate wear regime.

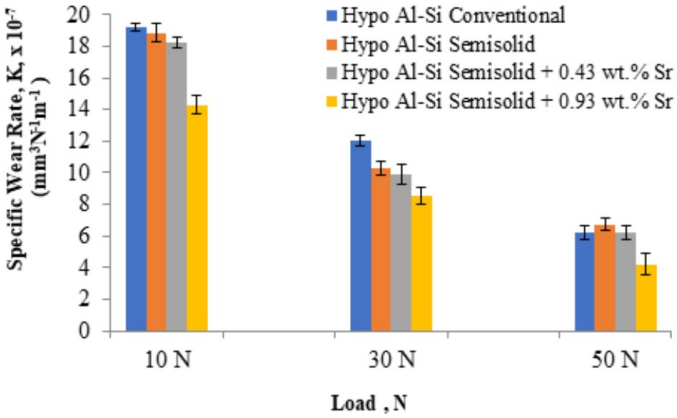


Fig. 8. Specific wear rate as a function of applied load for conventional, unmodified semisolid and modified Sr semisolid hypoeutectic Al-Si alloy

### 3.3.3. Friction coefficient, μ

At a load of 10 N, Fig. 9 depicts the coefficient of friction (COF) as a function of sliding distances for conventional, unmodified semisolid, and modified Sr semisolid hypoeutectic Al-Si alloys. At the start of the wear test, the alloys showed an increment line trend, which was followed by a fluctuating condition corresponding to the sliding distances, and then became steady. The decrease in COF was caused by the surface of the alloy becoming smoother and harder as a result of continued sliding. The COF fluctuation that occurred could be attributed to adhesion, oxidational wear, and debris accumulation at the interface of the pin and disc, that may reduce direct contact between the sample and countersurface surfaces, potentially lowering the COF even further. In addition, the friction coefficient at longer sliding distances appeared to fluctuate in the 0.25-0.35 range, possibly due to the entrapment of a large amount of wear debris between the contacts. This could be attributed to the presence of debris that was rolled into the interface of the sample [36].

At the start of the wear test, samples are in direct contact with the wear disc. Samples are rubbing and sliding (plastic deformation) against the wear counter disc and almost instantaneously generate friction force. Therefore, the friction coefficient is high at the beginning of the test. As the sliding distance increases,

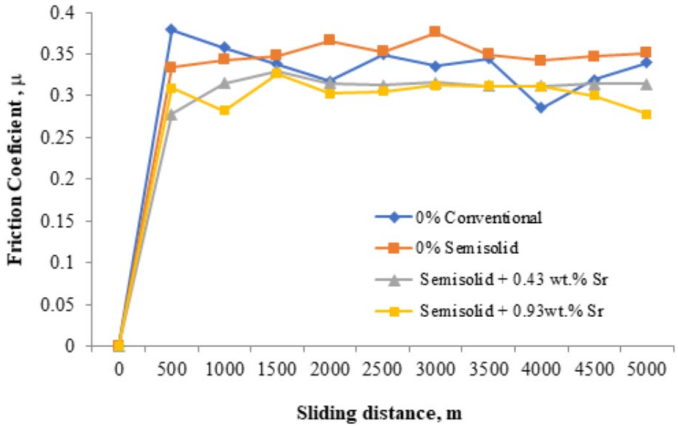


Fig. 9. Friction coefficient of conventional, unmodified semisolid and modified Sr semisolid hypoeutectic Al-Si alloy at 10 N load as a function of sliding distance

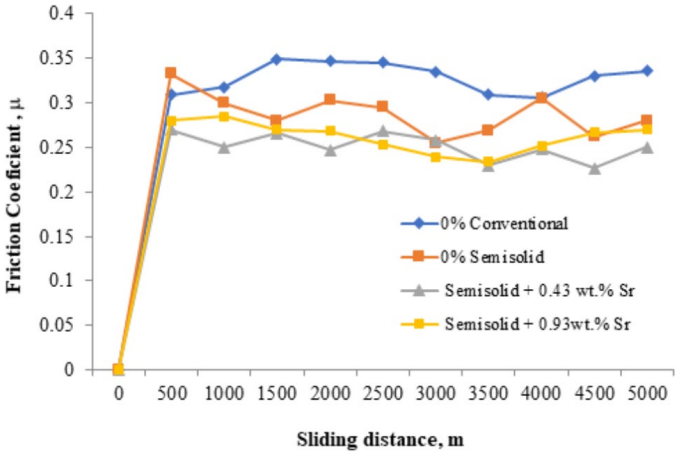


Fig. 10 Friction coefficient of conventional, unmodified semisolid and modified Sr semisolid hypoeutectic Al-Si alloy at 30 N load as a function of sliding distance

the oxide layer formed between the sample and the wear disc and reduced the direct contact of the sample and the disc [32]. Thus, increasing sliding resulted in reducing friction coefficient. The conventional and unmodified semisolid hypoeutectic Al-Si alloy showed higher friction coefficient. Higher friction coefficient means it requires more force to resist the relative motion of the rotating wear disc. Low wear resistance with high friction coefficient in conventional and unmodified semisolid hypoeutectic Al-Si alloy means ease of layer removal (delamination), because when the force of friction per unit area exceeds the shear strength of the sliding material, delamination occurs. The shear strength of the sliding material is strongly dependent on the hardness of the material. Upon addition of a modifier, eutectic silicon is refined and enhances its hardness (Fig. 4). Furthermore, the addition of Sr caused the formation of Sr block and needle shaped intermetallic phases that play the reinforcement role of hardening during wear test [37]. The intermetallic phases restrict the severe damage or wear on the substrate surface, lowering the friction coefficient.

Friction coefficients of conventional, unmodified semisolid and modified Sr semisolid hypoeutectic Al-Si alloy at applied load of 30 N and 50 N are shown in Fig. 10 and 11. Theoretically, as the load increases, the friction coefficient increases. This is because when the load increases, the temperature of the sample increases. Thus, soften the sample and lower the strength of the materials resulting in more wear loss and increase the contact area. At high load, more oxide layers formed between sample and wear disc, which protect the sample from further wear. Continuous wear will reduce the oxidation layer and then reform again. That might be the reason for fluctuating friction coefficient at high load [19].

Average friction coefficient against load is presented in Fig. 12. As the applied load increases, the friction coefficient decreases. At the higher load, an oxide layer may form on the surface due to rise in surface temperature and provide lubrication action that reduces friction. Presence of oxide layer shelter under layer new surface and reduces direct metallic contact. However, an abnormal trend appeared in 0.43 wt.% Sr. This might be due to the transition in wear from oxidative to adhesive, abrasive or

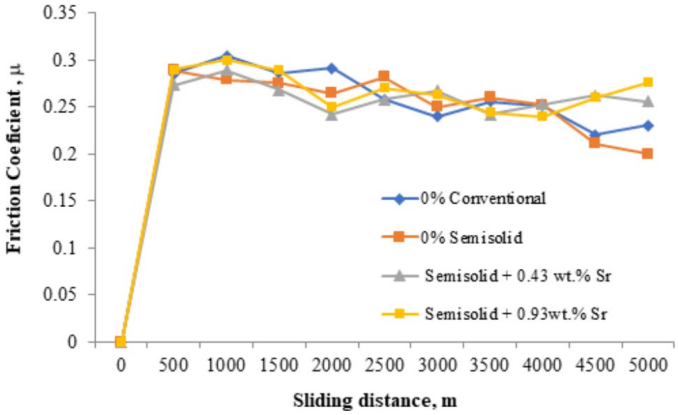


Fig. 11. Friction coefficient of conventional, unmodified semisolid and modified Sr semisolid hypoeutectic Al-Si alloy at 50 N load as a function of sliding distance

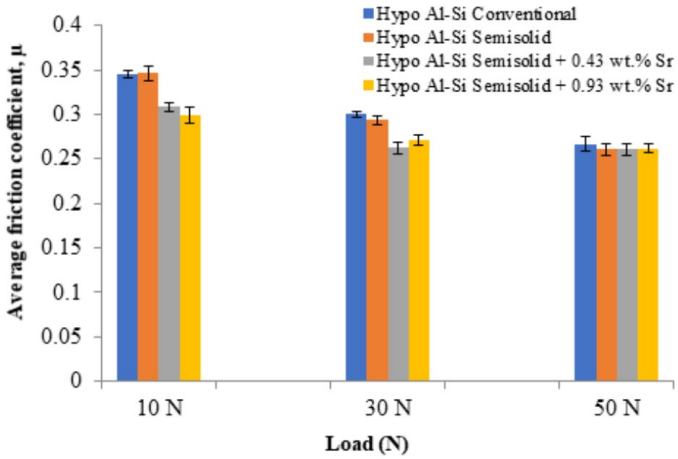


Fig. 12. Average friction coefficient of conventional, unmodified semisolid and modified Sr semisolid hypoeutectic Al-Si alloy as a function of applied load

other happened at applied load of 30 N [38]. The friction coefficient is inversely proportional to load applied upon the sample. The higher the load applied, the lower the friction coefficient.

### 3.3.4. Worn surface morphology

Fig. 13 and 14 show worn surface morphology of conventional, unmodified semisolid and semisolid hypoeutectic Al-Si alloy with various addition of Sr at applied load of 10 N and 50 N. Generally, the worn surface display typical wear features such as; micro grooves, micro cutting, craters and abrasive grooves [39-42]. The conventional, unmodified semisolid and modified semisolid hypoeutectic Al-Si alloys have a combination of adhesive and abrasion wear. Abrasion grooves seem to be wider in conventional and unmodified semisolid hypoeutectic Al-Si alloys and a bigger patch of crater formed. This could be due to coarse eutectic silicon that contributes to more wear loss. The coarser silicon particle from the contact surface is easily embedded into a softer alloy matrix and causes ploughing of the surface forming scratch marks.

Abrasion grooves seem narrower and smaller delaminated crater formed in the modified semisolid hypoeutectic alloys. This might be due to the fine eutectic silicon phase that is strongly bound with Al matrix that resists surface deformation [19]. For load comparison, the applied load of 50 N showed more severe wear as the samples may undergo severe plastic deformation, abrasion and higher degree of delamination. The loss of material in abrasive wear mainly takes place by two mechanisms: microcutting and ploughing. Hardness is regarded as the resistance property of material towards indentation or deformation. The greater is the depth of indentation, the lower is the hardness. Since abrasive wear mechanisms are involved in indentation, any factors that affect hardness will directly influence abrasive wear conditions [19,43].

Back scattered and EDX analysis were done on the wear surface of unmodified semisolid hypoeutectic Al-Si alloy at applied load 50 N as shown in Fig. 15. Based on the EDX results, high Al content was spotted on the grey region (B) whereas the bright particle consists of a high amount of iron (Fe). This Fe element comes from the wear disc (EN31 hardened steel) that adheres at sample surface which satisfies the adhesive wear behavior [44,45]. Adhesive wear of the cast Al alloy involved oxidation process, cyclic deterioration or combination of both processes [46]. The EDX results showed the presence of oxygen element indicated oxidation occured during the sliding. Ma et al. [47] 2008 have stated that several mechanisms such as metal transfer, film oxidation, debris formation and surface deterioration occurred during sliding.

Fig. 16 shows the back scattered and EDX analysis of modified semisolid hypoeutectic Al-Si alloy containing 0.93 wt.%. EDX analysis showed the presence of oxygen and iron which indicated that the modified alloys experience adhesive, abrasive and oxidative wear. Chandrashekharaiah et al. [31] have studied the worn surface of Al-12Si (LM-6). They have reported that the adhesive wear was dominant in the alloy without addition of grain refiner and modifier. However, an abrasive and oxidative wear was observed when the grain refiner and modifier are added to the same alloy. Studies by Liu et al. [48] 2011 have also reported that the abrasive wear is the main mechanism for unmodified alloys while abrasion wear occurs for modified alloy.

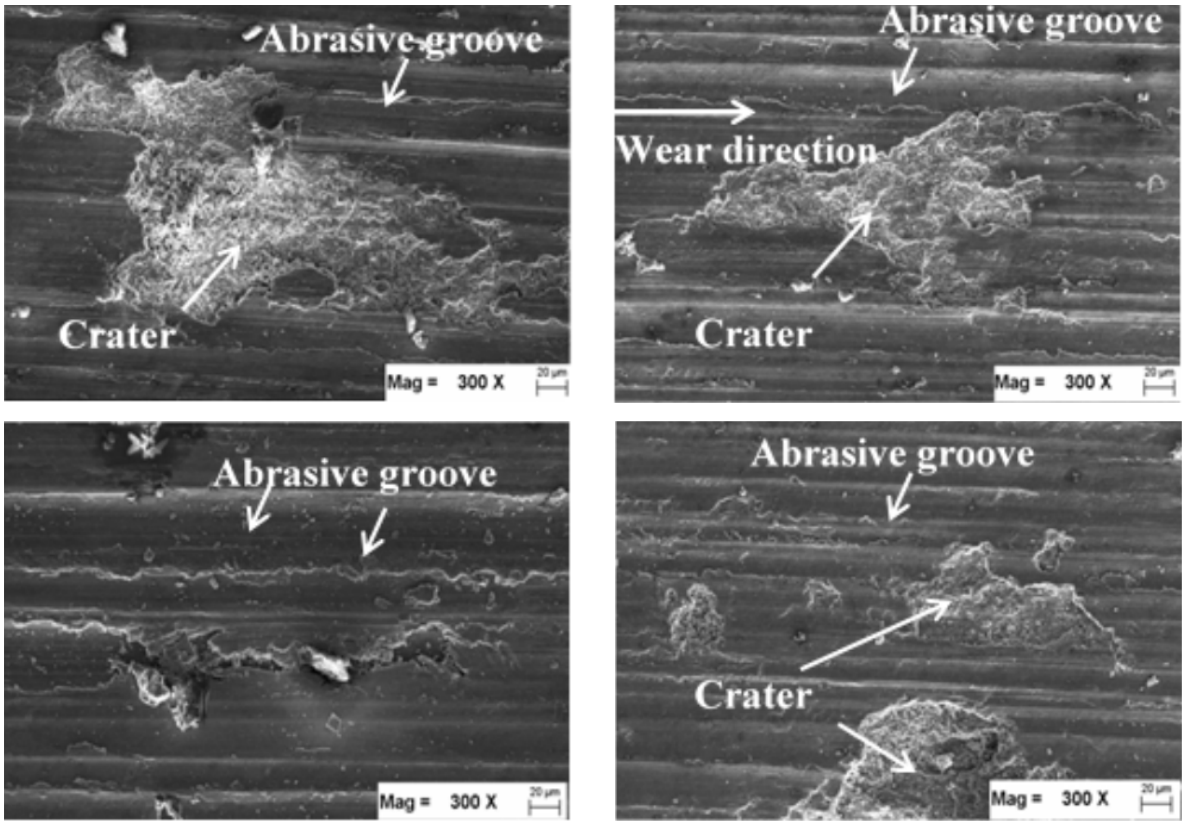


Fig. 13. Mirostructure of hypoeutectic Al-Si alloys at applied load of 10 N, (a) Conventional cast, 0 wt.% Sr, (b) semisolid cast, 0 wt.% Sr, (c) semisolid cast, 0.43 wt.% Sr, and (d) semisolid cast, 0.93 wt.% Sr

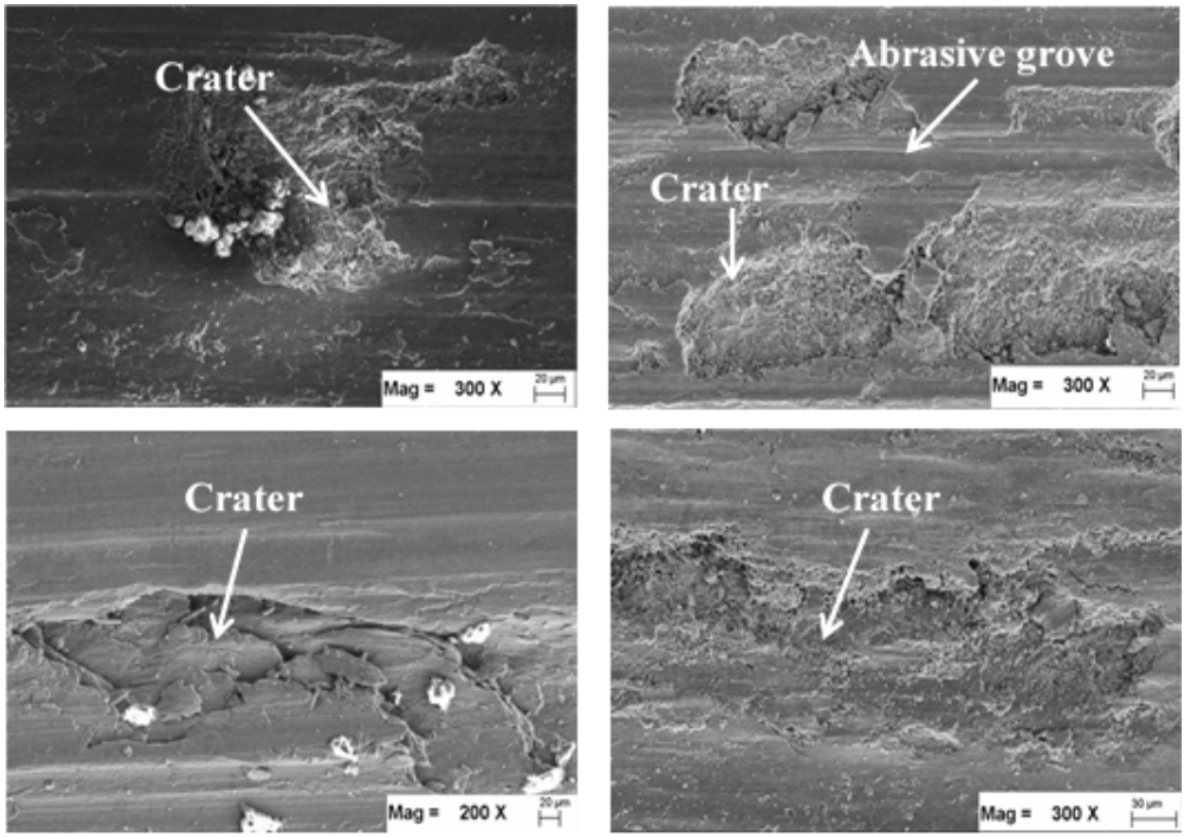


Fig. 14. Microstructure of hypoeutectic Al-Si alloys at applied load of 50N (a) Conventional cast, 0 wt.% Sr, (b) semisolid cast, 0 wt.% Sr, (c) semisolid cast, 0.43 wt.% Sr, and (d) semisolid cast, 0.93 wt.% Sr

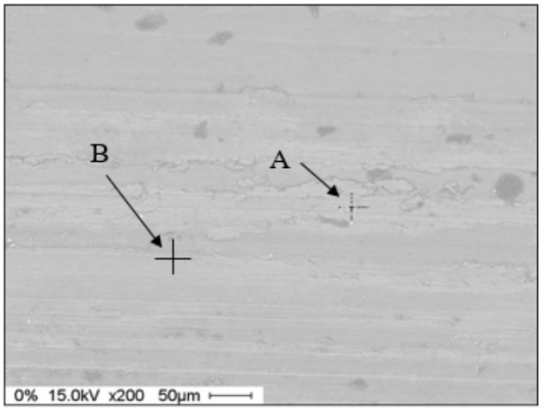


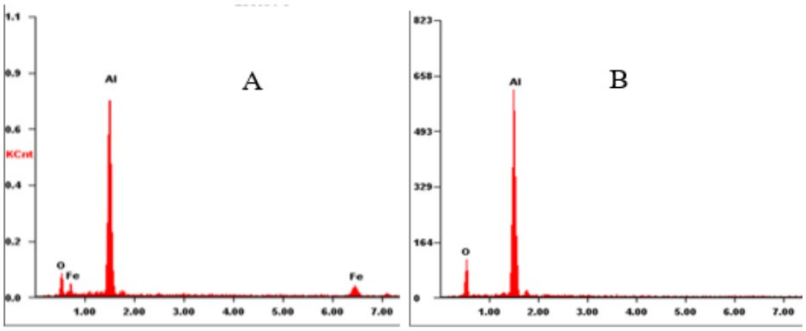


| Location | Composition (wt.%) | | |
|---|---|---|---|
| | Al | O | Fe |
| A | 62.54 | 10.82 | 26.65 |
| B | 79.75 | 20.25 | — |

Fig. 15. SEM image using backscattered electron and EDX analysis on worn surface of unmodified semisolid hypoeutectic Al-Si alloy at 50 N load

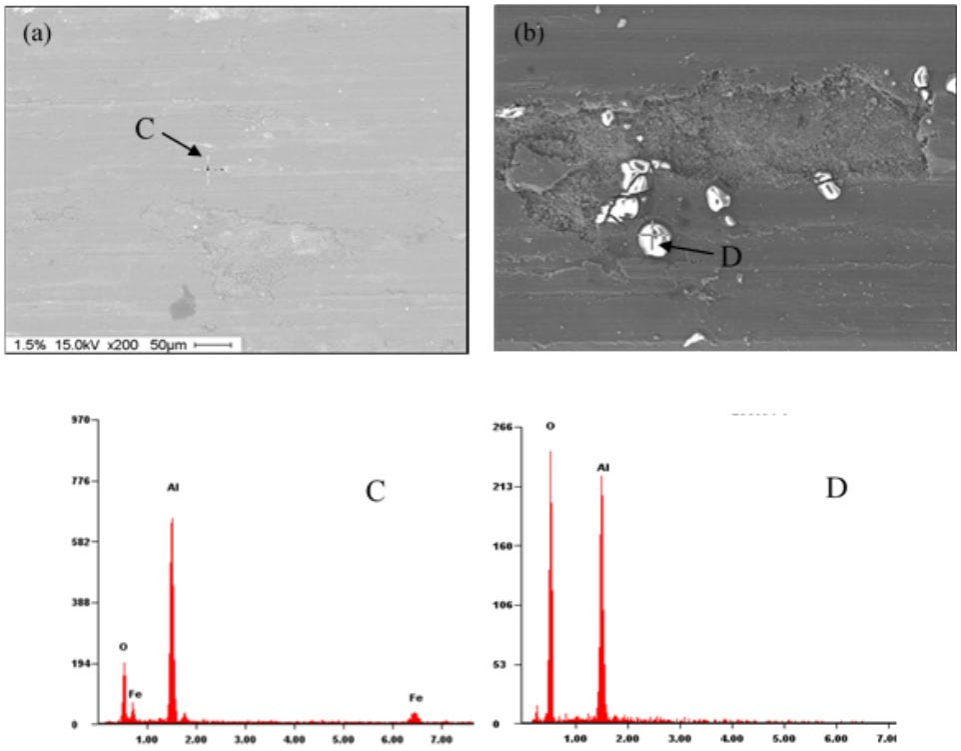


| Location | Composition (wt.%) | | |
|---|---|---|---|
| | Al | O | Fe |
| C | 51.70 | 23.69 | 24.61 |
| D | 51.54 | 38.68 | — |

Fig. 16. SEM image using backscattered electron and EDX result for semisolid hypoeutectic Al-Si alloy containing (a) 0.43 wt.%Sr and (b) 0.93 wt.%Sr

The higher oxygen was detected in modified alloy, then, it can be concluded that oxidative wear occurred more on modified alloy compared with unmodified alloy.

## 4. Conclusions

- The microstructure of the semisolid processed alloy contained fine α-Al globular structure with homogenous eutectic distribution, whereas the microstructure of the modified-Sr semisolid casting alloy consisted of fine α-Al globular structure and showed homogenous distribution, and refined eutectic structure.
- The hardness of modified-0.43wt.% Sr semisolid casting alloy improved by 17% compared to conventional casting. Addition of Sr more than 0.43 wt.% resulted in a high fraction of intermetallic compound containing Sr which reduced the hardness.
- The fine globular structure, homogeneous eutectic distribution, and refinement of the eutectic structure of the modified-Sr semisolid alloy resulted in high wear resistance. Abrasive wear is the primary wear mechanism for unmodified alloy (conventional alloy), whereas oxidative wear occurs on modified alloy.

Declaration of competing interest

The authors declare no conflict of interest.

**Acknowledgement**

The authors gratefully thank MYTRIBOS Industrial Grant, grant no. 304 / PBAHAN /6050471 /M171 for the funding.

## REFERENCES

[1] X. Yang, C. Xu, R. Zheng, S. Guan, C. Ma, Mater. Lett. **295**, 129850 (2021).
[2] D. Jiang, J. Yu, J. Mater. Res. Technol. **8** (3), 2930-2943 (2019).
[3] X.Y. Jiao, C.F. Liu, J. Wang, Z.P. Guo, J.Y. Wang, Z.M. Wang, J.M. Gao, S.M. Xiong, China Foundry **16**, 153-160 (2019).
[4] Y.S. Seo, L.M.M. Nasir, H. Zuhailawati, A.S. Anasyida, Advanced Materials Research **1087**, 488-492 (2015).
[5] Q. Zheng, L. Zhang, H. Jiang, J. Zhao, J. He, J. Mater. Sci. Technol. **47**, 142-151 (2020).
[6] A. Yasin, B. Murat, Material and Design **63**, 159-167 (2014).
[7] M. Javidani, D. Larouche, International Materials Reviews **59**, 132-159 (2014)
[8] Y.S. Lee, J.K. Jung, S.B. Kim, S.H. Kim, C.Y. Lim, H.W. Kim, W.K. Kim, S.K. Hyun, Materials Characterization **178**, 111256 (2021).
[9] G. Mao, H. Yan, C. Zhu, Z. Wu, W. Gao, Journal of Alloys and Compounds **806**, 909-916 (2019).
[10] Y. Birol, F. Birol, Wear **265**, 1902-1908 (2008).

[11] Z. Liu, W. Mao, W. Wang, Z. Zheng, T. Nonferr. Metal. Soc. **25**, 1419-1426 (2015).
[12] M.A.M. Arif, M.Z. Omar, Z. Sajuri, M.S. Salleh, T. Nonferr. Metal. Soc. **30** (2), 275-287 (2020).
[13] A. Kolahdooz, S.A. Dehkordi, J. Mater. Res. Technol. **8** (1), 189-198 (2019)
[14] L. Lasa, J.M. Rodriguez-Ibabe, Mat. Sci. Eng. A-Struct. **363** (1-2), 193-202 (2003).
[15] K.S. Alhawari, M.Z. Omar, M.J. Ghazali, M.S. Salleh, M.N. Mohammed, Procedia. Engineer. **68**, 186-192 (2013).
[16] M. Agarwal, R. Srivastava, Silicon-Neth. **11**, 355-366 (2019).
[17] M.M. Shehata, S. El-Hadad, M.E. Moussa, Int. J. Metalcast. **15**, 763-779 (2021).
[18] J. Gan, Y. Huang, W. Cheng, D.U. Jun, T. Nonferr. Metal. Soc. **30** (11), 2879-2890 (2020).
[19] A.K.P. Rao, K. Das, B.S. Murty, M. Chakraborty, Wear **261** (2), 133-139 (2006).
[20] A.K.P. Rao, K. Das, B.S. Murty, M. Chakraborty, Wear **257** (1-2), 148-153 (2004).
[21] C.Y. Yang, S.L. Lee, C.K. Lee, J.C. Lin, Wear **261** (11-12), 1348-1358 (2006).
[22] Y. Sui, Q. Wang, T. Liu, J. Alloy. Compd. **622**, 572-579 (2015).
[23] M.A. Abdelgnei, M.Z. Omar, M.J. Ghazali, M.A. Gebril, M.N. Mohammed, Int. J. Eng. Technol. **7**, 38-42 (2018).
[24] S.M. Jigajinni, K. Venkateswarlu, S.A. Kori, Met. Mater. Int. **19**, 171-181 (2013).
[25] S. Nafisi, R. Ghomashchi, Mat. Sci. Eng. A-Struct. **415** (1-2), 273-285 (2006).
[26] B.B. Stunova, Acta Polytechnica **52**, 26-34 (2012).
[27] M.A. Abdelgnei, M.Z. Omar, M.J. Ghazali, M.N. Mohammed, B. Rashid, Wear **442-443**, 203134 (2020).
[28] A.S. Anasyida, A.R. Daud, M.J. Ghazali, Mater. Design. **31** (1), 365-374 (2010).
[29] M. Elmadagli, T. Perry, A.T. Alpas, Wear **262** (1-2), 79-92 (2007).
[30] N.V. Thuong, H. Zuhailawati, A.A. Seman, T.D. Huy, B.K. Dhindaw, Mater. Design. 67, 448-456 (2015).
[31] T.M. Chandrashekharaiah, S.A. Kori, Ind. Tribol. Int. **42** (1), 59-65 (2009).
[32] S.A. Kori, T.M. Chandrashekharaiah, Wear **263** (1-6), 745-755 (2007).
[33] A. Pola, M. Tocci, P. Kapranos, Metals-Basel. **8** (3), 181 (2018).
[34] A.A. Seman, A.R. Daud, M.J. Ghazali, Ind. Lubr. Tribol. **65** (2), 135-140 (2013).
[35] E. Rabinowicz, Wear **100** (1-3), 533-541 (1984).
[36] K.S. Alhawari, M.Z. Omar, M.J. Ghazali, M.S. Salleh, M.N. Mohammed, Mater. Design. **76**, 169-180 (2015).
[37] J. Zhu, Z. Luo, S. Wu, H. Yan, Advances in Mechanical Engineering **10** (12), 1-10 (2018)
[38] M. Kathiresan, T. Sornakumar, Ind. Lubr. Tribol. **62** (6), 361-371 (2010).
[39] S. Padmanaban, R. Subramanian, J. Anburaj, K. Thillairajan, Materials Research. **23** (2), e20200063 (2020)
[40] N.V. Thuong, H. Zuhailawati, A.S. Anasyida, T.D. Huy, B.K. Dhindaw, International Journal of Materials Research **107**, 1-8 (2016).
[41] M.I. Abd El Aal, N. El Mahallawy, F.A. Shehataa, M. Abd El Hameeda, E.Y. Yoonc, H.S. Kim, Materials Science and Engineering A **527**, 3726-3732 (2010).
[42] R. Sharma, Anesh, D.K. Dwivedi, Mater. Sci. Eng. A. **408**, 274-80 (2005)
[42] C. Velmurugan, R. Subramanian, S. Thirugnanam, Ind. Lubr. Tribol. **64** (3), 138-146 (2012).
[43] P. Kumar, M.F. Wani. Jurnal Tribologi. **15**, 21-49 (2017).
[44] L. Cai, Z. Huang, W. Hu, Y. Chen, Z. Tan, M. Radovic, Ceramics International **47**, 6352-6361 (2021).
[45] A.S. Reddy, B.N.P. Bai, K.S.S. Murthy, S.K. Biswas, Wear **171** (1-2), 115-127 (1994).
[46] X.C. Ma, G.Q. He, D.H. He, C.S. Chen, Z.F. Hu, Wear **265** (7-8), 1087-1092 (2008).
[47] G. Liu, G. Li, A. Cai, Z. Chen, Mater. Design. **32** (1), 121-126 (2011).